THE ASTROPHYSICAL JOURNAL, 544:L149–L152, 2000 December 1

DISCOVERY OF A DISK-COLLIMATED BIPOLAR OUTFLOW IN THE PROTO–PLANETARY NEBULA IRAS 17106−3046[1]

SUN KWOK,[2] BRUCE J. HRIVNAK,[3] AND KATE Y. L. SU[2]
Received 2000 May 3; accepted 2000 September 8; published 2000 November 17

ABSTRACT

We report the discovery of a collimated bipolar outflow emerging from a visible disk around the proto–planetary nebula IRAS 17106−3046. The radius of the disk, estimated to be 2500 AU at a distance of 4 kpc, is too large for it to be a Keplerian disk created by accretion. The radial intensity profile of the disk suggests that it is consistent with an expanding torus. In contrast to the open-end, butterfly-like lobes commonly seen in bipolar planetary nebulae, the lobes of IRAS 17106−3046 have pointed ends, suggesting a recently formed jet breaking out of the lobes. IRAS 17106−3046 therefore could represent the earliest stage of the bipolar-shaping process during the transition from an asymptotic giant branch star to a planetary nebula.

Subject headings: ISM: jets and outflows — planetary nebulae: general — stars: AGB and post-AGB — stars: mass loss — stars: winds, outflows

1. INTRODUCTION

Although astrophysical jets in active galactic nuclei and young stellar objects (YSOs) are commonly assumed to be collimated by accretion disks, there have been very few examples where the jets and disks are directly imaged together. The discoveries of ansae in elliptical planetary nebulae (PNs; Balick et al. 1993) and of collimated outflows in bipolar and multipolar PNs (Sahai & Trauger 1998) have generated new interest in identifying the collimation mechanism in evolved stars (see Kastner, Soker, & Rappaport 2000). While it is now widely accepted that PNs evolve from asymptotic giant branch (AGB) stars over a period of a few thousand years through the interacting winds process, it is not clear how the largely spherical envelopes of AGB stars can be transformed into the aspherical (elliptical, bipolar, etc.) shapes of PNs in such a short time (Balick 1987). Proto–planetary nebulae (PPNs), objects in the short-lived transitional stage between the AGB and PN phases, could hold the key to answering this question.

Recent *Hubble Space Telescope* (*HST*) imaging studies have revealed a number of PPNs that display a bipolar morphology, therefore clearly demonstrating that the PN shaping must have started early in the PPN phase. For PPNs that are viewed edge-on, bipolar lobes separated by a dark lane can clearly be seen (Sahai et al. 1998; Kwok, Su, & Hrivnak 1998; Su et al. 1998; Hrivnak, Kwok, & Su 1999a). Even in cases of intermediate orientation where the two lobes are of unequal brightness, a dark gap is often present (K. Y. L. Su, B. J. Hrivnak, & S. Kwok 2000, in preparation; Ueta, Meixner, & Bobrowsky 2000). These observations provide indirect evidence that an equatorial density enhancement (disk or torus) is channeling the outflow.

In this Letter, we present the results of our *HST* imaging study of the remarkable bipolar lobes and the visible disk around the central star of the PPN IRAS 17106−3046. This object was initially selected as a PPN candidate based on its large infrared excess and cool *IRAS* color temperature, which indicated a detached circumstellar dust envelope (see Kwok 1993). An optical counterpart was identified, and more accurate coordinates were determined by ground-based 10 μm observations. These were followed up by subarcsecond visible imaging on the Canada-France-Hawaii Telescope, which revealed the object to be extended (Hrivnak et al. 1999b). These observations formed the basis for the higher resolution imaging with the *HST* presented here.

2. *HST* OBSERVATIONS

IRAS 17106−3046 was imaged using the Wide Field Planetary Camera 2 (WFPC2) on the *HST* (*HST* program 8210, PI: B. Hrivnak). The planetary camera was used with the wide-band filters F606W ($\langle\lambda\rangle$ = 603.1 nm, $\Delta\lambda$ = 150.2 nm) and F814W ($\langle\lambda\rangle$ = 804.0 nm, $\Delta\lambda$ = 154.0 nm). Observations were carried out on 1999 May 30. In each filter, three longer observations (500 s each) were made in a dithered pattern and two shorter observations (40 s each) at the same position. Standard procedures were used to remove the bias and dark counts from the images and to make flat-field corrections. The individual dithered images in each filter were then combined to remove cosmic rays and to improve the spatial resolution through "drizzling." The resulting spatial resolution (the FWHM of the point-spread function) was 0.″07 and 0.″07, respectively, in the shorter and longer F606W images and 0.″08 and 0.″09, respectively, in the shorter and longer F814W images.

3. ANALYSIS OF *HST* IMAGES

The images of IRAS 17106−3046 are shown in Figure 1. To bring out the details of the images, we have applied an unsharp mask filter, which increases the intensity contrast in the features. However, all of the main features discussed here are visible in the original drizzled images, and it is the original drizzled images that were used in the quantitative analysis.

These are the first *HST* images of IRAS 17106−3046, and they are truly remarkable. They show what appears to be a collimated bipolar outflow emerging from the center of a visible disk or torus, viewed at an intermediate angle. The outer edge of the disk is clearly seen. The pair of lobes are collinear, oriented at a position angle (P.A.) of 128° ± 1°, and the disk appears to be perpendicular to these (P.A. = 42° ± 4°). Due to the extreme redness of the star, these features are seen more

[1] This work was based on observations with the NASA/ESA *Hubble Space Telescope*, obtained at the Space Telescope Institute, which is operated by AURA, Inc., under NASA contract NAS5-26555.

[2] Department of Physics and Astronomy, University of Calgary, Calgary, ALB T2N 1N4, Canada; kwok@iras.ucalgary.ca, ysu@iras.ucalgary.ca.

[3] Department of Physics and Astronomy, Valparaiso University, Valparaiso, IN 46383-6493; bruce.hrivnak@valpo.edu.

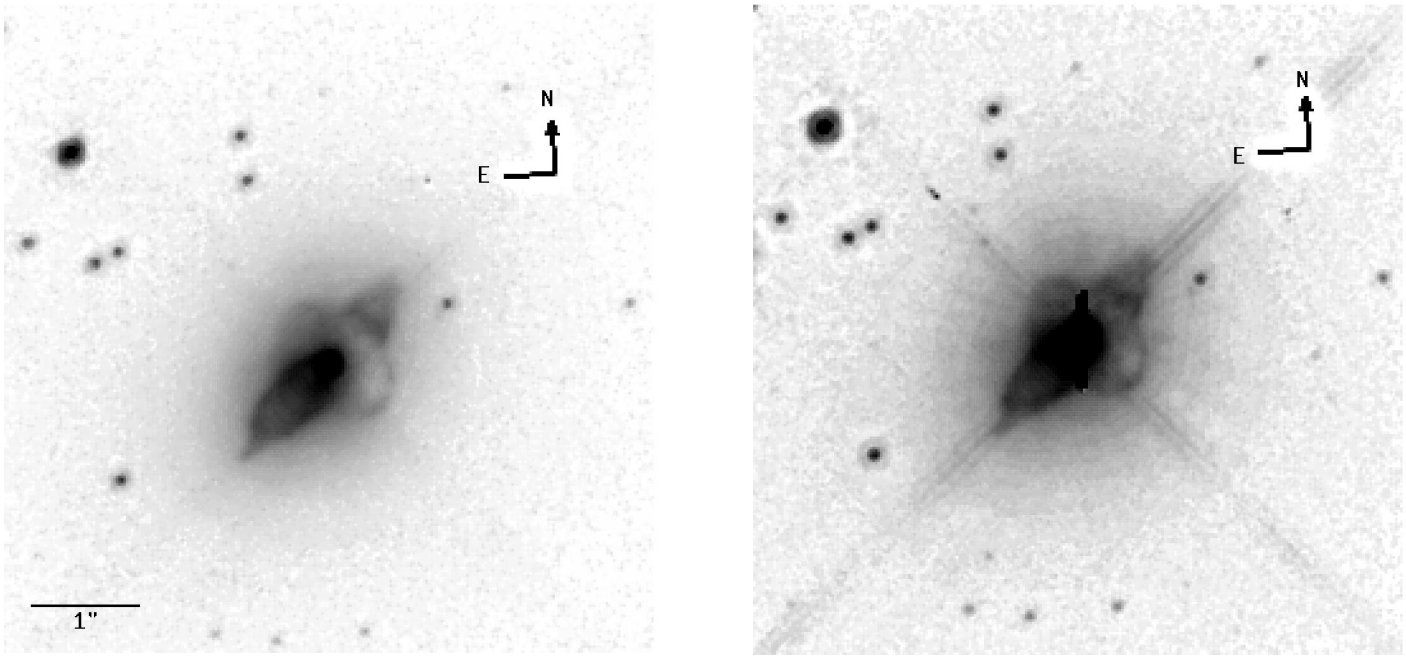

FIG. 1.—*HST* WFPC2 broadband F606W (*left*) and F814W (*right*) images of IRAS 17106−3046, with the application of an unsharp mask to increase the contrast in the images.

easily in the F606W image, but they are clearly present in both. These images provide the most direct evidence for a collimating equatorial disk in a PPN and are perhaps the best images of a collimating disk in any bipolar object.

3.1. *The Central Star, the Lobes, the Disk, and the Halo*

The central star is clearly resolved, although it is saturated in the longer exposure images in both filters. The position of the central star was determined from the shorter exposure images as R.A. (2000.0) = $17^{h}13^{m}51\overset{s}{.}6$ and decl. (2000.0) = $-30°49'39\overset{''}{.}82$. The southeastern (SE) lobe has the shape of a prolate ellipsoid, with dimensions of $1\overset{''}{.}20 \times 0\overset{''}{.}52$, and the northwestern (NW) lobe appears to be similar in shape but fainter and somewhat smaller. The difference in brightness of the two lobes is presumably the result of the viewing angle, with the brighter SE lobe pointing toward us and the NW lobe pointing away. Based on its general appearance, we suggest for it the name "Spindle Nebula." The two lobes appear brighter along their edges, which suggests that they are hollow cavities reflecting light from their walls. There appears to be a small feature extending radially outward from the tip of the SE lobe. Although the diffraction spikes are unfortunately oriented along the axis of the lobes, this feature does appear to be real. It may represent material beginning to "break out" from the confined lobe.

The disk in IRAS 17106−3046 displays a remarkable degree of circular symmetry with a well-defined edge. It has an apparent major axis of $1\overset{''}{.}27$ and a minor axis of $0\overset{''}{.}79$. If the disk is intrinsically circular and geometrically thin, then its minor-to-major axis ratio implies that the plane of the disk is inclined at an angle 38° to our line of sight.

A large elliptical halo surrounds the bipolar structure, with a size of $7\overset{''}{.}73 \times 6\overset{''}{.}59$, where the outer limit is defined as the place where the flux in the nebula has decreased to $3\sigma_{sky}$. The halo size is based on the F814W image, which has an overall higher signal-to-noise ratio (S/N). The halo is oriented at P.A. ≈ 129° and thus has the same orientation as the lobes. Since the halo is illuminated by scattered light, its shape reflects the distribution of photons and not necessarily the real geometry of the halo.

3.2. *Component Colors*

Standard aperture photometry was carried out on the object, using an elliptical aperture of $2\overset{''}{.}54 \times 1\overset{''}{.}75$ (major × minor axis) that approximately matches the size of the nebula in the F814 image. For this, the conservative value of $10\sigma_{sky}$ (i.e., S/N = 10) was used to define the outer extent of the nebulae in the sky-subtracted images. The derived magnitudes were transformed to the standard Johnson V and Cousins I_C systems using STSDAS synthetic photometry software, based on the effective blackbody temperature of the reddened photosphere. The standard magnitudes thus determined are $V = 15.99$ and $I_C = 12.70$.

The color $(V-I_C)$ image shown in Figure 2 clearly shows the relatively redder star and disk and the bluer reflection lobes, as expected for a bipolar reflection nebula with an obscuring equatorial disk. The central star can be seen to be the reddest of all, and its color is found to be $(V-I_C) = 3.9$ mag. The center of the SE lobe is bluer than the star by ~1.2 mag, with the edges of the lobe being bluer by an additional ~0.2 mag. The color of the disk is 0.4 mag bluer than that of the central star, which confirms that the disk is illuminated by the star. The color of the halo is 1.0 mag bluer than the star.

3.3. *Brightness Distribution in the Disk and Halo*

To investigate the intensity profile of the disk and halo, radial cuts were made from the central star through the disk and halo in both the F606W and F814W images. These are displayed in Figure 3. The intensity within $0\overset{''}{.}23$ was affected by the saturated central star and, in some cases, the bright reflection lobe. The intensity profiles toward the northeast (*solid lines*) are very similar in the different cuts. Toward the southwest, the intensity profiles (*dashed lines*) vary within the disk ($0\overset{''}{.}23 \leq r \leq 0\overset{''}{.}62$) and are consistently less than on the northeast

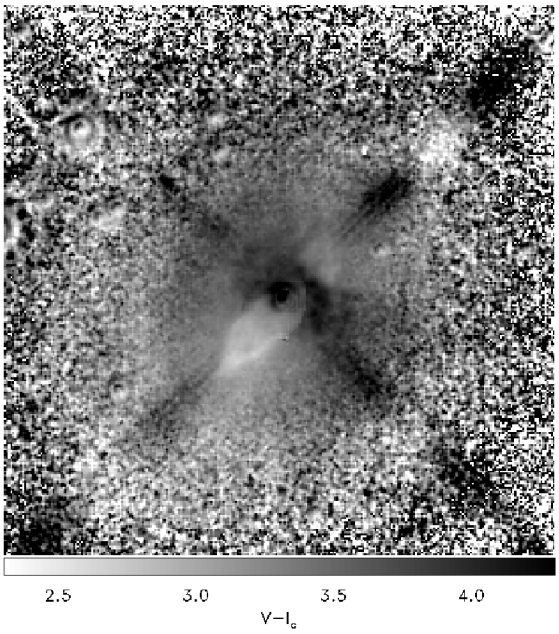

FIG. 2.—Color image ($V-I_C$) of IRAS 17106−3046. The redder the color, the darker the pixel. The central part of the nebula containing the saturated central star has been replaced by the corresponding short-exposure V and I images. A ($V-I_C$) color scale in units of magnitude is included along the bottom axis.

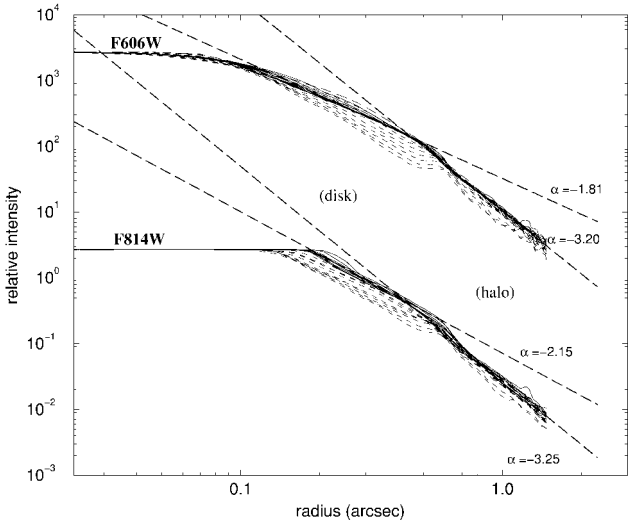

FIG. 3.—Intensity profile of IRAS 17106−3046. The cuts were made from P.A. = 15° to 55° (northeast) and from P.A. = 195° to 235° (southwest), at intervals of 5°. The cuts start from the position of the central star, and those toward the northeast direction are plotted with solid lines and those toward the southwest with dashed lines.

side. However, the profiles are approximately similar within the halo ($r \geq 0\farcs69$) on both sides. Apart from the localized obscuration apparent toward the west side, the brightness of the disk appears to be remarkably uniform.

It is obvious that the intensity profiles of the disk and halo follow different power laws ($I \propto r^{\alpha}$). The disk intensity (on the northeast side) is found to vary as a power law with $\alpha = -1.81$ in F606W and $\alpha = -2.15$ in F814W. The halo intensity is found to vary as a power law with $\alpha = -3.20$ in F606W and $\alpha = -3.25$ in F814W. Thus, the halo intensity in both images roughly follows $I \propto r^{-3}$. It is reasonable to assume that the halo is optically thin since it is far away from the central dense region. Since scattering in an optically thin spherical envelope with an r^{β} density law produces an $r^{\beta-1}$ intensity variation, the circumstellar envelope (the halo in the image) of IRAS 17106−3046 is therefore characterized by a $\rho \propto r^{-2}$ power law. This implies that the mass-loss rate was approximately constant with time at the end of the AGB phase.

The disk intensity follows a different power law, $I \propto r^{-2}$. If the disk is optically thick, then its intensity profiles simply reflects the intensity of the scattered light. Assuming a uniform-density disk with a thickness-to-radius ratio of 1/100, the disk will be optically thick if its mass exceeds $10^{-4}(D/4\ \mathrm{kpc})^2\ M_{\odot}$ (assuming a grain size of 0.1 μm, a grain density of 2.3 g cm^{-3}, and a dust-to-gas ratio of 3×10^{-3}). If the disk is optically thin, then the observed power law suggests that the density distribution has a smaller radial dependence ($\rho \propto r^{-1}$ if it is edge-on or $\rho \propto r^{0}$ if it is face-on). A density profile of $\rho \propto r^{-1}$ is generally interpreted as evidence for a rotating disk. However, an equatorial outflow can also produce similar density structures (see § 4).

4. DISCUSSION

4.1. *The Disk*

In previous studies of PPNs, the existence of a circumstellar disk was inferred either from visible images of bipolar PPNs, in which a dark lane was seen to separate the lobes (e.g., the Egg Nebula [Sahai et al. 1998] and IRAS 17441−2411 [Su et al. 1998]), or from mid-infrared images of a few PPNs, in which axially symmetric emission from circumstellar dust was observed (Meixner et al. 1997; Dayal et al. 1998). IRAS 17106−3046 was imaged in the mid-infrared (18.0 μm), but because of the limited spatial resolution (FWHM = $1\farcs4$; Meixner et al. 1999), it was not resolved. The *HST* images of IRAS 17106−3046 reported here show very clearly a circumstellar disk in scattered light, with ellipsoidal bipolar lobes emerging in a perpendicular direction, around a central star. This disk appears to have confined the direction of the bipolar outflow.

IRAS 04296+3429, another PPN that was identified from its infrared properties (Kwok, Volk, & Hrivnak 1989), also has a visible disk seen in scattered light. The main difference is that the disk in IRAS 04296+3429 has a more ringlike structure with a relatively large inner radius separating the disk from the star.

The most commonly invoked mechanism to produce a disk in an evolved star is the binary model. During a common envelope phase as the companion star spirals through the AGB atmosphere, preferential enhancement of mass loss can occur in the orbital plane and create a disk (Livio & Soker 1988). Another model involves preferential mass loss in a plane due to a very high rotation of the AGB star (Ignace, Cassinelli, & Bjorkman 1996; García-Segura et al. 1999 and references therein), perhaps induced by a close binary companion (Livio 1993). Assuming a stellar luminosity of 6000 $L_{\odot}$, we derived a distance of 4 kpc for IRAS 17106−3046 (K. Y. L. Su, B. J. Hrivnak, & S. Kwok 2000, in preparation). At that distance, the disk has a radius of $r = 4 \times 10^{16}$ cm, similar to the disk size found in IRAS 04296+3429 (Sahai 1999). These dimensions are too large for them to be Keplerian disks because the angular momentum per unit mass would be an order of magnitude greater than that of the binary systems that create them (Soker 2000). It is more likely that the observed disk in IRAS 17106−3046 represents an expanding torus. An optically thin equatorial torus expanding radially at constant velocity will have a density profile of $\rho \propto r^{-1}$, similar to the observed profile shown in Figure 3. Such a torus in PPNs could be the precursor of the expanding equatorial torus seen in some bipolar PNs (e.g., NGC 2420; López et al.

1998). Assuming an expansion velocity of 10 km s^{-1}, the dynamical age of the torus in IRAS 17106−3046 is 1300 yr.

4.2. *Collimation of the Outflow*

Hydrodynamic models have been advanced over the past decade that show that bipolar lobes can be produced as a fast tenuous wind from the central star expands into an ambient medium with an axially symmetric density profile (see recent review by Frank 1999 and references therein). If the equator-to-pole density ratio of the ambient medium is high enough, the oblique shock created by the interaction of the two winds could focus and collimate the outflow (Frank, Balick, & Livio 1996).

IRAS 17106−3046 appears to be an example of the morphology expected in this model. The ellipsoidal shape of the halo may be an indication of a latitude-dependent density in the final AGB mass loss, and the disk could represent the high-density contrast required in this shock-focused inertial confinement model. The small bright feature at the tip of the SE lobe may be evidence that a "jet" is beginning to break out of the collimated lobe (see Fig. 1 in Frank et al. 1996 and Fig. 3 in Borkowski, Blondin, & Harrington 1997).

Most bipolar PNs (e.g., NGC 6302 and NGC 2346) have open, untapered, fan-shaped lobes. The previously imaged bipolar PPNs (e.g., AFGL 2688, IRAS 17150−3224, and IRAS 17441−2411) have more confined lobes but still possess open ends. The lobes of IRAS 17106−3046 are more constrained and presumably represent an earlier stage in the evolution of bipolar lobes in PPNs. Simply based on morphology, it would appear that when the fast wind breaks through the ends of the lobes, it will produce a bipolar nebula with an appearance like the PN M2-9, which possesses bipolar ellipsoidal lobes with tattered, open ends. The morphology of IRAS 17106−3046 therefore provides useful constraints on the dynamical evolutionary models of bipolar nebulae.

It is interesting to note that the morphology of this PPN is also similar to that produced in models to explain the bipolar lobes of YSOs (Shu et al. 1994; Mellema & Frank 1997). Although the origins of the outflow are probably different between YSOs and PPNs, since YSO outflows are thought to be driven by the accretion *onto* the disk, YSOs and PPNs do share a common property in that they both involve isotropic or anisotropic winds expanding into an anisotropic medium. In this sense, the high-resolution imaging of the disk and the lobes in IRAS 17106−3046, as well as the emerging "jet," will provide important constraints on the collimation mechanism and on the dynamics of wind interactions for both PPNs and YSOs.

5. CONCLUSIONS

We have discovered a bipolar outflow emerging from a disk in the PPN IRAS 17106−3046. The outflow is embedded in a halo with a density structure of $\rho \propto r^{-2}$ and is likely the remnant of the stellar wind from the AGB phase. The disk itself has a density structure of $\rho \propto r^{-1}$ (if it is optically thin) and a size of $R \sim 3000$ AU, and it could represent an expanding torus formed late in the AGB evolution. Although the simultaneous presence of a disk/torus and bipolar lobes does not necessarily imply cause and effect, the near perpendicular orientation between the two in IRAS 17106−3046 is strongly suggestive that the disk plays a major role in the collimation process.

In contrast to the bipolar lobes commonly seen in PNs, the lobes in IRAS 17106−3046 have pointed ends, suggesting that the fast wind is just in the process of breaking out from the confining lobes. These observations give the most direct indications of the dynamical processes involved in the AGB–PPN–PN transition, and they pose strong constraints on the physical theories explaining the formation of bipolar outflows in the late stages of stellar evolution.

We thank Noam Soker for helpful discussions. Support for this work was provided by a grant to S. K. from the Natural Science and Engineering Research Council of Canada and by NASA grant GO-08210.01-97A to B. J. H. from the Space Telescope Science Institute, which is operated by the Association of Universities for Research in Astronomy, Inc., under NASA contract NAG5-26555. B. J. H. acknowledges the support of a University Research Professorship from Valparaiso University and the hospitality of the Steward Observatory, where part of this research was carried out.

REFERENCES

Balick, B. 1987, AJ, 94, 671
Balick, B., Rugers, M., Terzian, Y., & Chengalur, J. 1993, ApJ, 411, 778
Borkowski, K. J., Blondin, J. M., & Harrington, J. P. 1997, ApJ, 482, L97
Dayal, A., Hoffmann, W. F., Bieging, J. H., Hora, J. L., Deutsch, L. K., & Fazio, G. 1998, ApJ, 492, 603
Frank, A. 1999, NewA Rev., 43, 31
Frank, A., Balick, B., & Livio, M. 1996, ApJ, 471, L53
García-Segura, G., Langer, N., Różyczka, M., & Franco, J. 1999, ApJ, 517, 767
Hrivnak, B. J., Kwok, S., & Su, K. Y. L. 1999a, ApJ, 524, 849
Hrivnak, B. J., Langill, P. P., Su, K. Y. L., & Kwok, S. 1999b, ApJ, 513, 421
Ignace, R., Cassinelli, J. P., & Bjorkman, J. E. 1996, ApJ, 459, 671
Kastner, J. H., Soker, N., & Rappaport, S. A., eds. 2000, ASP Conf. Ser. 199, Asymmetrical Planetary Nebulae II: From Origins to Microstructures (San Francisco: ASP)
Kwok, S. 1993, ARA&A, 31, 63
Kwok, S., Su, K. Y. L., & Hrivnak, B. J. 1998, ApJ, 501, L117
Kwok, S., Volk, K., & Hrivnak, B. J. 1989, ApJ, 345, L51
Livio, M. 1993, in IAU Symp. 155, Planetary Nebulae, ed. R. Weinberger & A. Acker (Dordrecht: Kluwer), 279
Livio, M., & Soker, N. 1988, ApJ, 329, 764
López, J. A., Meaburn, J., Bryce, M., & Holloway, A. J. 1998, ApJ, 493, 803
Meixner, M., Skinner, C. J., Graham, J. R., Keto, E., Jernigan, J. G., & Arens, J. F. 1997, ApJ, 482, 897
Meixner, M., et al. 1999, ApJS, 122, 221
Mellema, G., & Frank, A. 1997, MNRAS, 292, 795
Sahai, R. 1999, ApJ, 524, L125
Sahai, R., & Trauger, J. T. 1998, AJ, 116, 1357
Sahai, R., et al. 1998, ApJ, 493, 301
Shu, F., Najita, J., Ostriker, E., Wilkin, F., Ruden, S., & Lizano, S. 1994, ApJ, 429, 781
Soker, N. 2000, MNRAS, 312, 217
Su, K. Y. L., Volk, K., Kwok, S., & Hrivnak, B. J. 1998, ApJ, 508, 744
Ueta, T., Meixner, M., & Bobrowsky, M. 2000, ApJ, 528, 861